Receptor for Activated C Kinase 1 promotes cervical cancer lymph node metastasis via glycolysis-dependent AKT/mTOR signaling pathway

Lixiu Xu
Xinjiang Medical University
Jinqiu Li
Xinjiang Medical University
Mikrban Tursun
Xinjiang Medical University
Yan Hai
Xinjiang Medical University
Hatila Tursun
Xinjiang Medical University
Batur Mamtimin
Xinjiang Medical University
Ayshamgul hasimu (axiangu75@126.com)
Xinjiang Medical University https://orcid.org/0000-0003-0499-3444

Research Article

Keywords: cervical cancer, Receptor for Activated C Kinase 1(RACK1), glycolysis, lymph node metastasis

Posted Date: January 17th, 2022

DOI: https://doi.org/10.21203/rs.3.rs-1249002/v1

Abstract

Background

Cervical cancer (CC), an aggressive squamous cell carcinoma, is characterized by early lymph node metastasis and extremely poor prognosis. We previously showed aberrant glycolysis in patients with CC. The upregulation of Receptor for Activated C Kinase 1 (RACK1) is associated with CC lymph node metastasis. However, its role in mediating aerobic glycolysis in CC lymph node metastasis remains unclear.

Methods

104 cervical cancer and 31 cervicitis tissue were enrolled. RACK1, insulin-like growth factor 1 receptor (IGF1R), POU class 2 homeobox 2 (POU2F2) and Hexokinase 2 (HK2) expression in cervical cancer patients were detected by Immunohistochemistry analysis. 1H-NMR experiment was used for metabolomics of cell supernatant after RACK1 knockdown. Tube formation assay, Transwell assay, determination of glucose consumption and lactate production assay were performed to detected MS751 and SiHa cells lymphangiogenesis, migration, invasion, glucose consumption and lactate production. Chromatin immunoprecipitation-PCR assay and Dual-Luciferase Reporter Assay was performed to detect the binding among POU2F2 and RACK1. Co-immunoprecipitation and Immunofluorescence staining were performed to detect the binding among RACK1 and GF1R. Xenograft footpad lymph node metastasis was performed using nude mice. Xenograft tumor and metastatic lymph node tissues of mice were experienced immunohistochemistry and hematoxylin–eosin staining.

Results

Here, ^{1}H-NMR analysis revealed significantly correlated RACK1 expression with glycolysis/gluconeogenesis pathway. Additionally, RACK1 knockdown inhibited aerobic glycolysis and lymphangiogenesis in vitro and suppressed CC lymph node metastasis in vivo. Furthermore, AKT/mTOR signaling was identified as a critical RACK1-regulated pathway that led to increased lymphangiogenesis in CC. Co-immunoprecipitation, immunofluorescence, and Western blot showed that RACK1 activated AKT/mTOR signaling by interacting with IGF1R. POU2F2 binds to RACK1 promoter and regulates RACK1 transcription, thus functionally contributing to glycolysis and lymphangiogenesis in CC. Importantly, administration of 2-deoxy-D-glucose, which attenuates glycolysis, inhibited RACK1-induced lymphangiogenesis in CC. The positive correlations between RACK1, IGF1R, POU2F2, and HK2 were further confirmed in CC tissues.

Conclusion

RACK1 plays an important role in CC tumor lymph node metastasis by regulating IGF1R/AKT/mTOR signaling mediated glycolysis pathways. Targeting the POU2F2/ RACK1/IGF1R/AKT/mTOR signaling pathway may provide a novel strategy for CC treatment.

Background

Cervical cancer (CC) is the fourth most common malignancy in women worldwide, and over the years, its increasing incidence and mortality have attracted considerable attention[1]. In particular, the incidence and mortality due to CC is high in the Xinjiang region of China[2]. Metastasis is responsible for more than 90% of cancer-related deaths, and there are few effective therapies for metastatic cancer [3]. Lymph node metastasis (LNM) and blood metastasis are common in the early and late stages of the disease, respectively. CC mainly metastasizes via the lymphatic vessels and by direct extension[4]. Therefore, preventing LNM is essential in CC therapy. Growing evidence suggests that LNM is a complex process involving mechanical forces within the tumor and host tissues as well as molecular factors initiated by tumor cell proliferation, cytokine production, and lymphangiogenesis[5]. Lymphangiogenesis involves the migration of endothelial cells into tumors and formation of new lymph vessels[6, 7]. However, lymphangiogenesis and its regulatory mechanisms in CC remain unclear.

Investigators have recently begun to view these metabolic changes as biomarkers for distinguishing tumor metastatic characteristics[8].Alteration in glucose metabolism, characterized by increased aerobic glycolysis (Warburg effect), is well established as one of the hallmarks of cancer[9], which contributes to tumor growth and metastasis by providing energy and substrates for biosynthesis[10, 11]. Our previous study tested plasma samples from patients with CC and normal controls using 1H-NMR based un-targeted metabolomics and found that glycolysis-related enzymes were upregulated in CC tissues[12]. This evidence indicates the importance of aerobic glycolysis in CC progression.

Receptor for Activated C Kinase 1 (RACK1) receptor, a multifunctional scaffolding protein, plays a functional role in nucleating cell signaling hubs and regulating protein activity and is also involved in modulating the migration and invasion of tumor cells[13]. A previous study showed that RACK1 is highly expressed in CC tissues and is positively associated with poor prognosis in patients with CC[14]. However, the metabolic significance and biological function of RACK1 in CC remain unclear. The above evidence led us to speculate that RACK1 promotes LNM by regulating glycolysis in CC.

In this study, we investigated whether RACK1 facilitates CC progression. RACK1 regulates glycolysis and lymphangiogenesis by interacting with IGF1R and activating AKT/mTOR signaling. In addition, POU2F2-mediated overexpression of RACK1 modulated the malignant progression of CC via sustained activation of the AKT/mTOR signaling pathway. Our findings reveal novel potential mechanisms in the CC LMN and provide promising new therapeutic targets. These new therapeutic targets and treatment options can effectively prevent the aggressiveness of CC.

Materials And Methods

Clinical samples

CC tissue specimens (n =104) and cervicitis tissue (NC, n =31) were collected from patients who underwent surgical resection at the First Affiliated Hospital of Xinjiang Medical University (Urumqi, Xinjiang, China) after obtaining written informed consent in accordance with the Ethics Committee of the First Affiliated Hospital of Xinjiang Medical University.

Cell culture

Human CC cell lines (MS751, SiHa, HeLa, and Caski), immortalized cervical epithelial cell line H8, and human lymphatic endothelial cells (HLECs)were purchased from Procell Life Science & Technology Co., Ltd. (Wuhan, China). SiHa, HeLa, and H8 cells were cultured in DMEM with 10% fetal bovine serum (FBS) (Gibco, USA). MS751 cells were cultured in MEM (containing NEAA) medium with 10% FBS, and the Caski cells were cultured in RPMI-1640 medium supplemented with 10% FBS. All cell lines were authenticated by STR profiling test to confirm their identities and in an incubator with 5% CO2 at 37 °C. Human lymphatic endothelial cells (HLECs) were obtained from Procell Life Science & Technology Co., Ltd. (Wuhan, China) and cultured in the ECM (ScienCell, CA, USA).

Lentiviral or plasmid transduction

To knockdown the expression of RACK1, a lentivirus containing short hairpin RNA (shRNA) targeting RACK1 or a non-target oligonucleotide was synthesized by Shanghai Genechem Co., Ltd. (Shanghai, China). The shRNA target sequences were 5'- AGCTGAAGACCAACCACAT-3' (shRACK1-1) and 5'- TGTGGTTATCTCCTCAGAT -3' (shRACK1-2). Stable cell lines were selected using 5 μg/mL puromycin (Sigma-Aldrich, USA), and knockdown efficiency was confirmed by western blot assays. The POU2F2 overexpression plasmid and control plasmid were purchased from Shanghai Genechem Co., Ltd. (Shanghai, China). Plasmid transfections were performed using Lipofectamine 3000 reagent (Invitrogen) according to the manufacturer's protocol. The OE target sequences are listed in Supplementary Table 1.

RNA extraction and quantitative real-time polymerase chain reaction (qRT-PCR)

RNA was extracted from CC cells using TRIzol reagent (Invitrogen, CA, USA). Reverse transcription of the extracted RNA was performed using a RevertAid First Strand cDNA Sythesis Kit (Thermo, MA, USA) following the manufacturer's instructions. PCR amplification was performed using QuantiNova SYBR Green PCR Kit (QIAGEN, Frankfurt, Germany). The relative expression of target genes was calculated using the $2^{-\triangle\triangle CT}$ method, and β-actin was used as a reference gene for normalization. Primer sequences used are listed in Supplementary Table 2.

Western blot analysis

Cells were lysed in radio-immunoprecipitation assay (RIPA) buffer containing protease/phosphatase inhibitor cocktail (Solarbio, Beijing, China). Proteins (30 μg) were separated in SDS-PAGE gels and transferred onto PVDF membrane (Millipore, USA). The membranes were then blocked with 5% milk and probed with primary and secondary horseradish-peroxidase- labeled antibodies. After washing thrice, the signaling was detected using an enhanced chemiluminescence detection system (ECL, Biosharp, Anhui, China). The primary antibodies used in this study are listed in Supplementary Table 3.

Immunohistochemistry (IHC) analysis

IHC analysis was performed on formalin-fixed, paraffin-embedded sections of clinical CC and mouse xenograft tissues. Paraffin-embedded tissue sections (4 μM) were rehydrated, blocked with 3% hydrogen peroxide, and treated with hot EDTA-mediated buffer. Next, primary antibodies were added and incubated overnight at 4°C. The results were determined using an IHC detection kit (ZSJQ-Bio, Beijing, China), according to the manufacturer's protocol. Staining intensity was scored independently by two observers. Briefly, the standard for the proportion of positive staining (1, < 5%, 2, 5–30%, 3, 30–70%, 4, > 70%) and staining intensity (0, no staining, 1, weak, 2, moderate, 3, strong) were multiplied for each observer and then averaged. The antibodies used and their corresponding experimental conditions are listed in Supplementary Table 3.

^{1}H NMR examination

The 1H NMR experiment was used for metabolomics analysis as described previously[12]. Briefly, cell supernatant samples were defrosted at room temperature. Each sample (200 μL) was mixed with 400 μl of saline (0.9% w/v NaCl in 20% v/v D2O and 80% v/v H_2O). The mixture at room temperature, and vortex-mixed followed by centrifugation (4°C, 10,000 rpm, 10 minutes). Then, 550 uL supernatant was transferred into a 5-mm NMR tube for 1H NMR (Varian 600 spectrometer with 599.93 MHz resonance frequency of 1H NMR). Transverse relaxation weighting experiments were performed as per the Carr–Purcell–Meiboom–Gill sequence with water peak suppression. Parameters were set as follows: relaxation delay 2.0 seconds, acquisition time 1.64 seconds, spectral width 10,000 Hz, which resulted in an acquisition time of 1.64 sec and a relaxation delay of 2 sec. Raw data were processed according to previous studies[15]. Briefly, 1H NMR spectra were processed and corrected for phase and baseline with Topspin 2.0 software (Brokers Biospin, Rheinstetten, Germany).we manually phased and baseline-corrected the 1H NMR spectra, which were referenced to the anomeric proton of α-glucose at δ 5.233 and the spectra were put into 2,834 integrated regions of 0.003 ppm. The regions of water resonance (δ 4.66–5.20) were excluded for eliminating the baseline effects. Then, we calculated the peak area of each bin. Normalization were performed with the software package SIMCA-P+11 (Umetrics Inc., Umea, Sweden) to compensate for the concentration differences among the samples.

Transwell migration assay of CC cells or HLECs

For the Transwell migration assay of CC cells, 2×10^4 cells were placed in the upper chamber of a Transwell (Corning, NY, USA). Basic medium containing 10% FBS was added to the lower chamber as chemoattractant and the cells were incubated at 37°C for 24 h. For HLECs migration, HLECs (1×10^5) were placed in the upper chamber with serum-free EGM, whereas the lower chamber was filled with conditioned medium derived from 1×10^5 CC cells with EGM medium at 1:1 ratio as chemo attractants and incubated at 37°C for 24 h. The cells attached to the reverse side of the membrane were stained with 0.1% crystal violet and counted under inverted microscope (Nikon E400, Tokyo, Japan) in randomly selected five fields.

Matrigel invasion assay

Matrigel-coated invasion chamber (BD Biosciences, NY, USA) was used to assess cell invasion. Briefly, 2×10^4 CC cells were seeded in the upper chamber of the Transwell insert in serum-free culture medium and cultured for 24-48 h. Penetrated cells were fixed with 4% paraformaldehyde and stained with 0.1% crystal violet. The number of penetrating cells in each group was counted under the inverted microscope (Nikon E400, Tokyo, Japan).

Determination of glucose consumption and lactate production

Glucose and lactate detection kits purchased from Nanjing Jiancheng Bioengineering Institute (Nanjing, China) were used to determine glucose and lactate concentrations before and after 24 h of CC cell culture, following the manufacturer's protocols.

Co-immunoprecipitation (Co-IP)

Co-IP assays were conducted to detect the interaction between RACK1 and IGF1R using protein A/G magnetic beads (Bimake, Shanghai, China). MS751 and SiHa cells were collected, lysed, and centrifuged at 4°C and 12,000 rpm for 20 min to obtain the supernatant, which was then mixed with primary antibody and incubated overnight at 4°C. Protein A beads were added and incubated for an additional 4 h. The beads were washed three times with PBST buffer for 5 min each time, 30 μL of loading buffer was then added and boiled for 5 min at 100°C. The supernatant was then used for western blot analysis.

Immunofluorescence staining

Cells were seeded on coverslips and incubated with antibodies specific for IGF1R and RACK1 at room temperature for 2 h. Next, the coverslips were incubated with Alexa Fluor 594 goat anti-mouse IgG and Alexa Fluor 488 goat anti-rabbit IgG for 2 h and stained with 4,6-diamidino-2-phenylindole (DAPI, Sigma, MO, USA) for 10 min. Randomized fields were captured using a microscope.

HLEC tube formation assay

Serum-free conditioned medium was prepared by culturing CC cells (1×10^7 cells per 10 cm dish) in 10 mL serum-free medium for 24 h. The media were collected and centrifuged at 1000 rpm for 5 min to

remove cell debris and stored at 4°C to concentrate the conditioned medium. HLECs were seeded into 24-well plates (precoated with 100 μL Matrigel) containing cell conditioned medium and incubated for 10-16 h. Tube formation was quantified by measuring the total length of tube structures or the number of branch sites/nodes in three random fields.

Dual luciferase reporter assay

A plasmid with the RACK1 promoter was designed and constructed by Shanghai GeneChem Co., Ltd. (Shanghai, China). The wild-type and mutant sequences of the RACK1 promoter, named GV712-RACK1-WT and GV712-RACK1-mut, were amplified and cloned into the GV712-basic vector. The cells were then collected and lysed 48 h after transfection, and luciferase activity was detected using the Dual-Luciferase Reporter Assay System (Promega, WI, USA) and a luciferase assay kit (Bio-Vision Technologies, PA, USA).

Chromatin immunoprecipitation-PCR (ChIP-PCR) analysis

The chromatin immunoprecipitation assay was performed according to the manufacturer's instructions and protocols. Cells were (1×10^7) fixed with 1% formaldehyde for 10 min at room temperature, and the fixation was stopped with 0.125 M glycine, the cell lysis buffer was then added, and the samples were sonicated to generate 200–1000 bp fragments. The resulting cell lysates were immunoprecipitated using a POU2F2 antibody (Sanying, Wuhan, China) and analyzed using RT-PCR. Anti-POU2F2 antibody and primers used for the PCR assay of ChIP samples are listed in Supplementary Table 1.

Xenograft model

All animal experiments were approved by the Ethics Committee of the First Affiliated Hospital of Xinjiang Medical University. Xenograft models were established as previously described[16]. Female BALB/c nude mice were purchased from Beijing Vital River Laboratory Animal Technology Co., Ltd. For the xenograft LNM model, 5×10^5 cells were inoculated into the footpads of the mice. The mice were sacrificed by cervical dislocation four weeks after the first injection of tumor cells. Footpad tumors and popliteal lymph nodes were removed by hematoxylin and eosin (HE) staining.

Statistical analysis

The results are presented as the mean ± standard error of the mean (SEM). IBM SPSS Statistics for Windows, version 23.0(IBM Corp., Armonk, NY, USA) and GraphPad (5.0 version) were used for the statistical analyses. Two-tailed Student's t-test and one-way ANOVA with Tukey's post-hoc test were used for comparisons between two or multiple groups, respectively. The relationships between RACK1 expression and clinicopatho-logical characteristics were evaluated using Pearson's $\chi 2$ test or Fisher's exact test. Correlations between measured variables were analyzed using Spearman's rank correlation analysis. $P < 0.05$ was considered statistically significant (*, $p < 0.05$, *, $p < 0.01$, **, $p < 0.001$, ***).

Results

RACK1 is highly expressed in CC cell lines and regulates CC cell migration, invasion, and lymphangiogenesis in vitro

We first evaluated the implications of RACK1 expression in patients with cervical cell carcinoma (CC) using online data. Analysis of the GEO database (GEO Submission: GSE6791) demonstrated that patients with CC had higher RACK1 expression than normal cervical tissues (Figure S1A). However, GSE9750 showed that RACK1 was downregulated in CC tissues compared to normal cervical tissues (Figure S1A). Next, the analysis of GSE26511 showed that RACK1 expression was not significantly correlated with LNM ($p = 0.0706$) (Figure S1B). Although it did not achieve statistical significance in CC and normal cervical tissues, the expression of RACK1 was positively correlated with LNM. We first examined the expression of RACK1 mRNA and protein in the normal human cervical cell line H8 and the four CC cell lines (HeLa, SiHa, Caski, and MS751) (Figure 1A and B). RACK1 exhibited higher expression in CC cell lines than in normal cervical cells, especially in MS751 cells, which had the highest expression of RACK1 and is a CC cell with high metastatic potential. These results suggest that RACK1 is a potential biomarker for human CC with LMN.

To study the biological function of RACK1, we chose two CC cell lines, MS751 and SiHa, as cellular models. Non-specific control shRNA (shNON) and RACK1-shRNA (shRACK1-1 and shRACK1-2) were transfected into MS751 and SiHa cells, respectively, and stable cell lines were established after puromycin treatment. These results showed that knockdown of RACK1 effectively downregulated RACK1 mRNA and protein expression in the MS751 and SiHa cell lines (Figure 2C and D). When we performed transwell assays in MS751 and SiHa cells, we observed that the inhibition of RACK1 by its specific shRNA decreased the invasion and migration of MS751 (Figure 2E) and SiHa (Figure S1C) cells compared to that of the control group transfected with shNON. Notably, there was weaker invasion and migration of MS751cells than SiHa cells. We speculated that MS751 cells promoted lymphatic endothelial cell migration to acquire advantage of lymphatic metastasis. Transwell assay showed that knockdown of RACK1 on MS751 cells inhibited the migration of HLECs (Figure 2F) and suppressed the lymphangiogenesis (Figure 2G). These results demonstrated that RACK1 acts as an important tumor promoter in the aggressiveness of CC cells.

RACK1 regulates the glycolysis in CC cells

Metabolic changes play important roles in regulating cellular aggressiveness[17]. Considering that RACK1 is a crucial regulator of cellular function, we hypothesized that RACK1 downregulation may contribute to metabolic reprogramming in CC cells. To define the metabolic alterations induced by RACK1, we first examined the differential metabolites of RACK1 knockdown in MS751 and SiHa cells using ^{1}H-NMR analysis. Table S4 shows 19 species of differential metabolites in shRACK1/MS751 cells compared to shNON/MS751 cells, of which 6 species were increased and 13 were decreased. Table S5 shows 24 species of differential metabolites in shRACK1/SiHa cells compared to shNON/SiHa cells, of which 16

were increased and 8 were decreased. Moreover, there were 17 species of common differential metabolites in shRACK1/MS751 and shRACK1/SiHa cells, of which 12 were upregulated and 5 were downregulated (Supplementary Table 6). Importantly, we found a significant correlation between RACK1 downregulation and glycolysis/gluconeogenesis in common differential metabolites using MetaboAnalyst 5.0, online analysis (https://www.metaboanalyst.ca/) (Figure 2A and Supplementary Table 7). Aerobic glycolysis facilitates tumor metastasis with elevated glucose uptake and lactate production [18, 19]. Next, we used glucose uptake and lactate production as glycolysis indices in CC cells. Our results showed that knockdown of RACK1 in MS751 and SiHa cells significantly decreased the glucose uptake by 63% and 56%, and lactate production by 69% and 63% revealed that RACK1 knockdown significantly suppressed glucose consumption and lactate production (Figure 2B). Consistent with these observations, the glycolytic enzymes Hexokinase 2 (HK2), lactate dehydrogenase A (LDHA), Glucose transporter 1 (GLUT1), and Pyruvate kinase M2 (PKM2) were downregulated by RACK1 (Figure 2C-E). These results indicate that RACK1 can enhance glycolysis by affecting the expression of relevant metabolic enzymes.

RACK1 affects glycolysis and lymphangiogenesis by interacting with IGF1R in CC cells

We searched for candidate factors that interacted with RACK1 using Hitpredict (http://www.hitpredict.org/) and 263 candidate factors that may interact with RACK1 were identified. These factors were further mapped using Genemania (http://genemania.org/), and four overlapping factors were considered as candidate factors that interacted with RACK1 (Figure 3A). IGF1R has been reported to regulate the expression of glycolysis-related genes in various cancers[20]. A previous study identified that RACK1 interacts with IGF-1R to influence its biological function in tumor cells [21, 22]. We subsequently investigated whether RACK1 interacted with the IGF1R in CC cell lines. The interaction between RACK1 and IGF1R was analyzed and demonstrated through a protein–protein molecular docking experiment. Co-IP analysis of CC cells demonstrated exogenous interaction of RACK1 with IGF1R (Figure 3B and Figure S2A). Immunofluorescence results of colocalization of RACK1 and IGF1R in the cytoplasm of CC cells are consistent with the results of the Co-IP assay (Figure 3C).

Previous research has verified that the AKT/mTOR signaling pathway is a target of IGF1R in cancer cells [23]. Therefore, we hypothesized that RACK1 can activate AKT/mTOR signaling by interacting with the IGF1R in CC cells. The expression patterns of the key genes involved in AKT/mTOR signaling, AKT phosphorylation (p-AKT), total AKT (AKT), and mTOR phosphorylation (p-mTOR), were further validated by analyzing their post-transcript levels through Western Blot analysis (Figure 2C). We found that RACK1 downregulation significantly decreased the binding between RACK1 and IGF1R and reduced the phosphorylation of AKT and mTOR, although total AKT and mTOR expression was not markedly changed. Thus, we hypothesized that RACK1 might positively regulate AKT/mTOR signaling by interacting with the IGF1R. Next, we explored the functional significance of the IGF1R in the metabolic and metastatic roles of RACK1 in CC cells using IGF1. We found that IGF1 promoted AKT/mTOR signaling activity in CC cells. Moreover, our results indicated that IGF1 regulated the activation of AKT/mTOR signaling in CC cells in a time-dependent manner. Western blot results indicated that the

activation of AKT phosphorylation and mTOR phosphorylation was significantly increased by IGF1 at 6 h, 12 h, and 24 h (Figure 3D, F, S2B, and D). Therefore, we chose 24 h as the administration time for IGF1 in subsequent experiments. We found that the activation of AKT/mTOR signaling by IGF1 partially reversed the biological effects of RACK1. As expected, the reduction in invasion and migration (Figure 3G and S2E) of CC cells and inhibited the migration of HLECs (Figure 3H) and lymphangiogenesis (Figure 3I) induced by RACK1 knockdown was largely reversed by IGF1 treatment. Next, we sought to determine whether the activation of AKT/mTOR signaling by IGF1 is involved in RACK1-mediated glycolytic metabolism. Glucose uptake and lactate production were increased by IGF1 treatment (Figure 3J and S2F). Western Blot analyses confirmed that the expression of glycolysis-related enzymes in RACK1 knockdown cells returned to levels comparable to those in control cells (Figure 3D, F, S2B, and D). Hence, our results suggest that RACK1 contributes to IGF1R-mediated aerobic glycolysis and lymphangiogenesis of CC cells.

RACK1 influences glycolysis and lymphangiogenesis through activating IGF1R/AKT/mTOR signaling

Previous research has verified that the IGF1R/AKT/mTOR signaling pathway is correlated with aerobic glycolysis in cancer cells[24]. We further determined whether IGF1R/AKT/mTOR is involved in regulating CC cell glycolysis. Therefore, we performed a rescue experiment to analyze the relationship between IGF1R and the AKT/mTOR signaling pathway. Rapamycin (Rapa), an mTOR inhibitor, efficiently attenuated IGF1-induced promotion of glycolysis in CC cells, as revealed by the level of glucose uptake and lactate production (Figure 3J and S2F). Decreased phosphorylation of mTOR and glycolysis-related enzyme expression induced by IGF1 was abrogated by Rapa (Figure 3E, F, S2C, and D). Furthermore, we validated that RAPA could reverse the effects of IGF1 in promoting invasion and migration of CC cells (Figure 3G and S2E), HLECs migration (Figure 3H) and lymphangiogenesis (Figure 3I). Collectively, these results indicate that, in CC cells, RACK1 promotes glycolysis, migration, invasion and lymphangiogenesis via IGF1R/AKT/mTOR signaling.

RACK1 is a direct target of POU2F2

Cancer metabolism is regulated by a complex network composed of different factors in various contexts rather than by straightforward single-pathway manipulation[25]. Next, we explored the molecular mechanism by which RACK1 mediates IGF1R/AKT/mTOR signaling pathway activation and aerobic glycolysis. We also explored the upstream regulatory machinery of RACK1. Three software systems (GUSC, HUMANTFDB, and PROMO) were used to predict potential complementary base pairing between RACK1 and transcription factors (TFs). Only POU2F2 coexisted in the data from the three software packages (Figure 4A). A previous study revealed that POU2F2 is expressed at significantly higher levels in CC[26]. Recent studies have described the important roles of POU2F2 in glucose metabolism related to the oncogenic AKT/mTOR signaling pathway[27]. The JASPAR database predicted a POU2F2 response element in the RACK1 promoter (Figure 4B). To confirm whether POU2F2 binds to the 3’-UTR of the RACK1 mRNA, a dual-luciferase reporter assay was performed. The relative luciferase activity was significantly increased in CC cells co-transfected with GV238-RACK1-3’UTR and the POU2F2 mimic.

Mutation of the 3'-UTR of RACK1 mRNA abrogated these repressive effects (Figure 4C and S3A), suggesting that POU2F2 binds to the 3'-UTR of RACK1 mRNA. Furthermore, we used ChIP-PCR assays to demonstrate that POU2F2 could bind to the RACK1 promoter in CC cells (Figure 4D and S3B). Next, we performed rescue experiments by transfecting MS751 and SiHa cells with a POU2F2-overexpression plasmid to further explore the effects of POU2F2 on RACK1/IGF1R/AKT/mTOR signaling pathway activation. We found that RACK1 expression levels increased to an extent similar to that in shNON cells upon POU2F2 overexpression (Figure 4E, S3C and D). Moreover, we validated that POU2F2 overexpression abrogated the inhibitory effects of RACK1 on migration and invasion CC cell(Figure 4F and S3E), HLECs migration (Figure 4G) and lymphangiogenesis (Figure 4H).Decreased phosphorylation of AKT, phosphorylation of mTOR, and glycolytic enzyme expression induced by RACK1 knockdown were rescued by POU2F2 overexpression (Figure 4E, S3C and D).We also found POU2F2 overexpression efficiently restored the level of glucose uptake and lactate production by RACK1-induced inhibition in CC cells (Figure 4I and S3F).Based on these results, POU2F2 is required for RACK1-mediated aggressiveness and aerobic glycolysis by activating IGF1R/AKT/mTOR signaling.

RACK1 promoted CC invasion, migration, and lymphangiogenesis through activating aerobic glycolysis

Increased aerobic glycolysis has been coupled with various malignant phenotypes of cancer cells, including metastatic CC [28, 29]. To test whether the promoting effects of RACK1 on CC cell aggressiveness were dependent on aerobic glycolysis, 2-DG, a glycolytic inhibitor, was added to the cell culture medium. The presence of 2-DG led to a decrease in invasion and migration of CC cells (Figure 4F and S3E), HLECs migration (Figure 4G) and lymphangiogenesis (Figure 4H) in RACK1 re-expression upon POU2F2 overexpression. These results imply that RACK1 may exert oncogenic functions in CC cells by activating CC cell aggressiveness in a glycolysis-dependent manner.

RACK1 promotes LNM and aerobic glycolysis of CC in vivo

To study the effects of RACK1 on the growth and LNM of CC in vivo, we injected sh-RACK1/SiHa, sh-NON/SiHa, sh-RACK1/MS751, and sh-NON/MS751 cells into the footpads of mice to establish a xenograft model. After four weeks, the mice were sacrificed, the size of the footpad tumors was measured, and the inguinal lymph nodes were removed. Strikingly, sh-RACK1/SiHa and sh-RACK1/MS751 injections prominently inhibited the metastasis in the primary tumor of the inguinal LNs of nude mice compared with the sh-NON/SiHa and sh-NON/MS751 groups (Figure 5A and S4A). Since the lentiviral plasmids were labeled with green fluorescent protein (GFP), transfected cancer cells that metastasized into the lymph nodes could be identified by IHC staining of GFP (Figure 5A and S4A). Subsequently, we calculated LNM rates in the different groups. This rate was lower in the sh-RACK1/MS751 (25%, 2/8) and sh-RACK1/SiHa (37.5%, 3/8) groups than sh-NON/SiHa (87.5%, 7/8) and sh-NON/MS751 (87.5%, 7/8) groups. We found that the tumor size and volume of lymph node was smaller in sh-RACK1/MS751 and sh-RACK1/SiHa than sh-NON/SiHa and sh-NON/MS751 (Figure 5D, E, S4D, and E). Moreover, IHC analysis showed a lower density of lymphatic vessels, as indicated by podoplanin (PDPN) in sh-RACK1/SiHa and sh-RACK1/MS751 groups than in sh-NON/SiHa and sh-NON/MS751 groups (Figure 5B and S4B),

suggesting that RACK1 markedly induces LN metastasis in vivo. Furthermore, the downstream glycolytic enzymes LDHA, PKM2, HK2, and LDHA were lower in tissues from the sh-RACK1/SiHa and sh-RACK1/MS751 group than that in the sh-RACK1/SiHa and sh-RACK1/MS751 groups (Figure 5C and S4C). Collectively, these findings reveal that downregulation of RACK1 inhibits aerobic glycolysis and the aggressiveness of CC in vivo.

RACK1 expression is correlated with POU2F2, IGF1R and HK2 expression in clinical CC specimens

To determine the relationship between RACK1 expression and aerobic glycolysis in clinical CC specimens, we examined paraffin-embedded tissues from 104 clinical CC specimens using IHC experiments. The results showed that RACK1 was more highly expressed in CC tissues than in cervicitis tissues. Moreover, RACK1 overexpression was significantly correlated with tumor differentiation and positive lymph nodes but was not correlated with tumor size or FIGO stage (Figure S5A and Table 1). We subsequently profiled the expression of RACK1, POU2F2, IGF1R, and HK2 using IHC staining. Consistent with our observations in tumor cell lines and xenograft models, the distribution and intensity of RACK1 were positively correlated with POU2F2, IGF1R, and HK2 expression in CC tissues (Figure S5B-D). As shown in Figure 6, CC samples had RACK1 strong expression, which correlated with strong POU2F2, IGF1R, and HK2 expression (representative case 1, Figure 6A). Accordingly, CC samples with RACK1 medium expression levels had medium levels of POU2F2, IGF1R, and HK2 (representative case 2, Figure 6B). CC samples with RACK1 weak expression had weak levels of POU2F2, IGF1R, and HK2 (representative case 3, Figure 6C). CC samples with RACK1 negative expression levels had negative expressions of POU2F2, IGF1R, and HK2 (representative case 4, Figure 6D). Altogether, these results further suggest that the molecular mechanism by which RACK1 induces aerobic glycolysis and LN metastasis include the activation of the POU2F2-mediated IGF1R/AKT/mTOR signaling pathway in patients with CC.

Discussion

LNM confers a poor prognosis on CC patients, as effective treatment modalities are currently lacking[30]. Therefore, the elucidation of the molecular mechanisms underlying LNM may provide clinical preventive and therapeutic strategies for patients with CC and LNM. However, the precise mechanism underlying LNM in CC remains largely unknown. This study determined the specific expression of RACK1 in CC and its key role in promoting LNM. In our study, POU2F2 directly regulated RACK1, and RACK1 interacted with IGF1R. Therefore, RACK1 links POU2F2 to the IGF1R/AKT/mTOR signaling pathway. The interaction of RACK1 with the POU2F2/IGF1R/AKT/mTOR pathway promoted CC glycolysis, and the subsequent regulatory effects on cell LNM were dependent on glycolysis (Figure 7). These findings indicate that RACK1 plays a pivotal role in CC progression, suggesting RACK1 as a potential therapeutic target in the treatment of CC.

RACK1 has been described as one of seven critical network nodes with specific properties that play an important role in the invasion and distant metastasis of tumors [31, 32]. Wu et al. [13] discovered high and specific expression of RACK1 in metastatic CC tissue, but Wang et al. [33] revealed decreased RACK1

expression in CC tissues compared to normal cervical tissues. In the current study, the GEO database showed that RACK1 expression was upregulated or downregulated in CC. RACK1 was upregulated in cancer tissues in GSE6791; but RACK1 was downregulation in cancer tissues in GSE9750. Above all, the potential molecular mechanisms of RACK1 in CC are unclear. In this study, we demonstrated that RACK1 is upregulated in CC tissues and cell lines, especially in CC cells with high metastatic potential (MS751 cell lines). Moreover, knockdown of RACK1 inhibited tumor cell invasion, migration, and lymphangiogenesis and reduced glycolysis in vitro. Furthermore, the knockdown of RACK1 decreased the rate of LNM in vivo. These data suggest that RACK1 may represent a potential molecular target for clinical intervention in patients with CC and LNM.

Alterations in intracellular metabolic intermediates that accompany can-cer-associated metabolic reprogramming have profound effects on tumor progression[34]. Accumulating evidence has demonstrated that glucose is required as an energy source and that cellular glycolysis levels are crucial for cancer metastasis[11, 35]. Our previous study used 1H NMR spectroscopy to analyze plasma samples from CIN patients, CC patients, and normal controls, and we reported that aberrant glycolysis-related enzymes differed among the normal, CIN, and cancer groups[12]. In addition, RACK1 is involved in glucose metabolism during cancer metastasis[36]. PER1 depends on the PER1/RACK1/PI3K/AKT pathway to promote glycolysis, and regulation of the cell me-tastasis depends on glycolysis in oral squamous cell carcinoma (OSCC) [37]. RACK1 in-teracts with FGFR to promote the phosphorylation of PKM2, thereby increasing tumor metastasis via glycolysis in lung squamous cell carcinomas[18]. Thus, we investigated whether RACK1 could modulate glycolysis to promote LNM in CC. In our study, 1H NMR analysis indicated notable correlations between RACK1 downregulation and the glycolysis/gluconeogenesis pathways. Consistent with the above findings, we found that the knockdown of RACK1 decreased the intracellular glucose uptake and lactate pro-duction by downregulating the expression of key glycolytic enzymes in CC cells, such as GLUT1, PKM2, HK2, and LDHA. Therefore, inhibiting aberrant glycolysis by targeting RACK1 may be a new strategy for treating CC patients with LNM. However, based on 1H NMR analysis, RACK1-induced cell metabolic changes involve not only aerobic glycolysis, but glutamine metabolism is also prominently regulated by RACK1, which we aim to investigate in a future study.

Another important finding in the present study was that RACK1 activated the AKT/mTOR pathway by interacting with the IGF1R in CC. The IGF1R plays a primary role in regulating glucose metabolism and promotes cell invasion and metastasis[38]. A few studies have demonstrated the pro-tumor properties of IGF1R in CC[39, 40]. IGF1R is considered to be one of regulators of the Akt/mTOR pathway. Kiely et al. [41] identified RACK1 as an IGF1R interacting protein that negatively affects the activation of the AKT pathway. However, Zhang et al. [22]found that the effect of RACK1 on IGF1R induced the activation of AKT but failed to observe a change in Akt activation in MCF7 cells. In a recent study, RACK1 interacted with IGF1R, enabling activation of the AKT pathway in favor of prostate cancer[42] and renal cell carcinoma[43] progression. Our experiments demonstrated that RACK1 interacted with IGF1R and knockdown of RACK1 could decrease the binding capacity between RACK1 and IGF1R, leading to inactivation of the AKT/mTOR pathway in CC cells. Another study showed that aberrant activation of the AKT/mTOR pathway is

associated with cancer progression[44, 45]. Moreover, the glycolytic processes governed by the AKT/mTOR pathway are crucial in cancer metastasis [46], but the activation of the AKT/mTOR pathway mediated by RACK1 in glycolytic processes and LNM in CC remains unknown. To elucidate the mechanism by which the AKT/mTOR pathway regulates CC cell lymphangiogenesis and glycolysis, we performed rescue experiments. These results showed that IGF1 restored activation of the AKT/mTOR pathway and promoted cancer cell lymphangiogenesis and glycolysis in CC. Based on these results, we suggest that RAPA, an mTOR inhibitor, inhibits CC cell progression and glycolysis by decreasing mTOR phosphorylation. These findings indicate that RACK1 constitutively activates the AKT/mTOR pathway, which is crucial for the progression and glycolysis of CC, and expands the current knowledge on AKT/mTOR pathway regulation in CC. However, IGF1R is not the only factor of RACK1 because at least three factors were predicted to interact with RACK1 by bioinformatic analysis. The precise molecular mechanisms by which RACK1 interacts with the IGF1R in CC remain unclear. Gaining a deeper understanding of the minimal binding motif in RACK1 required for its interaction with the IGF1R in future studies is important.

Recently, a growing number of studies have reported high expression of POU2F2 in tumor tissues, and have even described the role of POU2F2 in promoting tumorigenesis and metastasis[47]. POU2F2 is a member of the POU TF family that coordinates nu-merous cell responses from internal cues of pluripotency and differentiation to external stimuli of proliferation and apoptosis in a time-and cell-specific manner[48]. Moreover, recent studies showed that the expression of POU2F2 significantly promote CC cell pro-liferation[26]. However, abnormal POU2F2 expression of the LMN in CC remains unclear. Bioinformatic analysis showed that POU2F2 is the only upstream regulator of RACK1 and is predicted to form complementary base pairings with RACK1. We found a POU2F2 binding sequence (5’-TTATTTTGCATAG-3’) in the RACK1 promoter by JASPAR database prediction. We found that POU2F2 overexpression restored the expression of RACK1 in shRACK1 cells. Here, for the first time, we discovered and confirmed that through direct binding to the RACK1 promoter region at sites −681 to −693, POU2F2 transcriptionally activated RACK1, thus stimulating the AKT/mTOR signaling pathway and promoting CC lymphangiogenesis and glycolysis. 2-DG, a glycolysis inhibitor, added to CC cells, stably overexpressed POU2F2 for functional rescue experiments. We found that the inhibition of glycolysis showed promising suppressive effects on migration and invasion with RACK1 re-expression, upon overexpressing POU2F2 in CC cells, indicating the critical role of aberrant glycolysis in RACK1-induced LNM in CC. Furthermore, high expression of RACK1 was correlated with lymph nodes in clinical CC specimens and was positively correlated with POU2F2, IGF1R, and HK2 in CC tissues. These results indicate that the POU2F2/RACK1/IGF1R/AKT/mTOR pathway may be a promising biomarker for CC. In addition, our findings provide a new understanding of the upstream regulatory machinery of RACK1, and a novel treatment strategy aimed at preventing RACK1-mediated CC LNM.

Conclusions

In summary, our findings demonstrate that RACK1 interacts with IGF1R to activate the AKT/mTOR pathway (Figure 7), which has important implications for the underlying mechanism of cell lymphangiogenesis depending on RACK1-mediated glycolysis. Thus, our study not only identifies a crucial mechanism of cross-talk between RACK1 and glycolysis that promotes LNM but also provides a potential early diagnostic biomarker and therapeutic target for CC patients with LNM.

Abbreviations

CC
Cervical cancer
RACK1
Receptor for Activated C Kinase 1
IGF1R
Insulin-like growth factor 1 receptor
POU2F2
POU class 2 homeobox 2
AKT
Protein Kinase B
mTOR
Mammalian Target of Rapamycin
HK2
Hexokinase 2
LDHA
Lactate dehydrogenase A
GLUT1
Glucose transporter 1
PKM2
Pyruvate kinase M2
PDPN
podoplanin
2-DG
2-deoxy-D-glucose
LNM
Lymph node metastasis
IHC
Immunohistochemistry
^{1}H NMR
^{1}H nuclear magnetic resonance
shRNA
Short hairpin RNA

Co-IP
Co-immunoprecipitation
Rapa
Rapamycin
ChIP
Chromatin immunoprecipitation.

Declarations

Ethics approval and consent to participate

This study was approved by the Ethics Committee of the First Affiliated Hospital of Xinjiang Medical University (authorization number: IACUC-20180223-128) and was conducted in accordance with the tenets of the Declaration of Helsinki.

Consent for publication

Not applicable.

Competing interests

The authors declare that they have no competing interests.

Funding

This study was funded by the Xinjiang Uygur Autonomous Region Science and Technology Plan Project, PR China.

Authors' contributions

Conceived and designed the experiments: LX and AH. Performed the experiments: LX, JL, MT, and HT. Analysis and interpretation of data: LX, JL, YH, and BM. Wrote the manuscript: LX and AH. All authors read and approved the final manuscript.

Acknowledgements

Not applicable.

Availability of data and materials

The datasets used and/or analyzed during the current study are available from the corresponding author on reasonable request.

Author details

[1] Department of Basic Medicine, Xinjiang Medical University, Urumqi 830000, Xinjiang, People's Republic of China.[2] Department of Gernal Medicine, Xinjiang Medical University, Urumqi 830000, Xinjiang, People's Republic of China.[3] Department of Pharmacy, Medical University of Xinjiang, Urumqi 830000, Xinjiang, People's Republic of China,

References

1. Kagabu M, Yoshino N, Saito T, et al. The efficacy of a third-generation oncolytic herpes simplex viral therapy for an hpv-related uterine cervical cancer model[J]. Int J Clin Oncol. 2021;26(3):591–7.
2. Husaiyin S, Jiao Z, Yimamu K, et al. Thinprep cytology combined with hpv detection in the diagnosis of cervical lesions in 1622 patients[J]. PLoS One. 2021;16(12):e0260915.
3. Yang H, Kuo YH, Smith ZI, et al. Targeting cancer metastasis with antibody therapeutics[J]. Wiley Interdiscip Rev Nanomed Nanobiotechnol. 2021;13(4):e1698.
4. Federico C, Sun J, Muz B, et al. Localized delivery of cisplatin to cervical cancer improves its therapeutic efficacy and minimizes its side effect profile[J]. Int J Radiat Oncol Biol Phys. 2021;109(5):1483–94.
5. Swartz MA, Lund AW. Lymphatic and interstitial flow in the tumour microenvironment: Linking mechanobiology with immunity[J]. Nat Rev Cancer. 2012;12(3):210–9.
6. Fagiani E, Lorentz P, Bill R, et al. Vegf receptor-2-specific signaling mediated by vegf-e induces hemangioma-like lesions in normal and in malignant tissue[J]. Angiogenesis. 2016;19(3):339–58.
7. Liu D, Zeinolabediny Y, Caccuri F, et al. P17 from hiv induces brain endothelial cell angiogenesis through egfr-1-mediated cell signalling activation[J]. Lab Invest. 2019;99(2):180–90.
8. Park MK, Zhang L, Min KW, et al. Neat1 is essential for metabolic changes that promote breast cancer growth and metastasis[J]. Cell Metab. 2021;33(12):2380–97.e2389.
9. Vaupel P, Schmidberger H, Mayer A. The warburg effect: Essential part of metabolic reprogramming and central contributor to cancer progression[J]. Int J Radiat Biol. 2019;95(7):912–9.
10. Luo P, Zhang C, Liao F, et al. Transcriptional positive cofactor 4 promotes breast cancer proliferation and metastasis through c-myc mediated warburg effect[J]. Cell Commun Signal. 2019;17(1):36.
11. Yang J, Ren B, Yang G, et al. The enhancement of glycolysis regulates pancreatic cancer metastasis[J]. Cell Mol Life Sci. 2020;77(2):305–21.
12. Hasim A, Aili A, Maimaiti A, et al. Plasma-free amino acid profiling of cervical cancer and cervical intraepithelial neoplasia patients and its application for early detection[J]. Mol Biol Rep. 2013;40(10):5853–9.
13. Wu H, Song S, Yan A, et al. Rack1 promotes the invasive activities and lymph node metastasis of cervical cancer via galectin-1[J]. Cancer Lett. 2020;469:287–300.

14. Wu J, Meng J, Du Y, et al. Rack1 promotes the proliferation, migration and invasion capacity of mouse hepatocellular carcinoma cell line in vitro probably by pi3k/rac1 signaling pathway[J]. Biomed Pharmacother. 2013;67(4):313–9.
15. Hasim A, Ali M, Mamtimin B, et al. Metabonomic signature analysis of cervical carcinoma and precancerous lesions in women by (1)h nmr spectroscopy[J]. Exp Ther Med. 2012;3(6):945–51.
16. Liu D, Li C, Trojanowicz B, et al. Cd97 promotion of gastric carcinoma lymphatic metastasis is exosome dependent[J]. Gastric Cancer. 2016;19(3):754–66.
17. Bower AJ, Li J, Chaney EJ, et al. High-speed imaging of transient metabolic dynamics using two-photon fluorescence lifetime imaging microscopy[J]. Optica. 2018;5(10):1290–6.
18. Li HM, Yang JG, Liu ZJ, et al. Blockage of glycolysis by targeting pfkfb3 suppresses tumor growth and metastasis in head and neck squamous cell carcinoma[J]. J Exp Clin Cancer Res. 2017;36(1):7.
19. Wan J, Liu Y, Long F, et al. Circpvt1 promotes osteosarcoma glycolysis and metastasis by sponging mir-423-5p to activate wnt5a/ror2 signaling[J]. Cancer Sci. 2021;112(5):1707–22.
20. Lenz G, Hamilton A, Geng S, et al. T-darpp activates igf-1r signaling to regulate glucose metabolism in trastuzumab-resistant breast cancer cells[J]. Clin Cancer Res. 2018;24(5):1216–26.
21. Hermanto U, Zong CS, Li W, et al. Rack1, an insulin-like growth factor i (igf-i) receptor-interacting protein, modulates igf-i-dependent integrin signaling and promotes cell spreading and contact with extracellular matrix[J]. Mol Cell Biol. 2002;22(7):2345–65.
22. Zhang W, Zong CS, Hermanto U, et al. Rack1 recruits stat3 specifically to insulin and insulin-like growth factor 1 receptors for activation, which is important for regulating anchorage-independent growth[J]. Mol Cell Biol. 2006;26(2):413–24.
23. Lin T, Yang Y, Ye X, et al. Low expression of mir-99b promotes progression of clear cell renal cell carcinoma by up-regulating igf1r/akt/mtor signaling[J]. Int J Clin Exp Pathol. 2020;13(12):3083–91.
24. Ellis BC, Graham LD, Molloy PL. Crnde, a long non-coding rna responsive to insulin/igf signaling, regulates genes involved in central metabolism[J]. Biochim Biophys Acta. 2014;1843(2):372–86.
25. Sun T, Liu Z, Yang Q. The role of ubiquitination and deubiquitination in cancer metabolism[J]. Mol Cancer. 2020;19(1):146.
26. Zhou L, Xu XL. Long non-coding rna arap1-as1 facilitates the progression of cervical cancer by regulating mir-149-3p and pou2f2[J]. Pathobiology. 2021;88(4):301–12.
27. Yang R, Wang M, Zhang G, et al. Pou2f2 regulates glycolytic reprogramming and glioblastoma progression via pdpk1-dependent activation of pi3k/akt/mtor pathway[J]. Cell Death Dis. 2021;12(5):433.
28. Guler OC, Torun N, Yildirim BA, et al. Pretreatment metabolic tumour volume and total lesion glycolysis are not independent prognosticators for locally advanced cervical cancer patients treated with chemoradiotherapy[J]. Br J Radiol. 2018;91(1084):20170552.
29. Cegla P, Burchardt E, Roszak A, et al. Influence of biological parameters assessed in [18f]fdg pet/ct on overall survival in cervical cancer patients[J]. Clin Nucl Med. 2019;44(11):860–3.

30. Osaku D, Komatsu H, Okawa M, et al. Re-classification of uterine cervical cancer cases treated with radical hysterectomy based on the 2018 figo staging system[J]. Taiwan J Obstet Gynecol. 2021;60(6):1054–8.
31. Duan F, Wu H, Jia D, et al. O-glcnacylation of rack1 promotes hepatocellular carcinogenesis[J]. J Hepatol. 2018;68(6):1191–202.
32. Han H, Wang D, Yang M, et al. High expression of rack1 is associated with poor prognosis in patients with pancreatic ductal adenocarcinoma[J]. Oncol Lett. 2018;15(2):2073–8.
33. Wang J, Chen S. Rack1 promotes mir-302b/c/d-3p expression and inhibits ccno expression to induce cell apoptosis in cervical squamous cell carcinoma[J]. Cancer Cell Int. 2020;20:385.
34. Torresano L, Nuevo-Tapioles C, Santacatterina F, et al. Metabolic reprogramming and disease progression in cancer patients[J]. Biochim Biophys Acta Mol Basis Dis. 2020;1866(5):165721.
35. Li S, Zhu K, Liu L, et al. Lncarsr sponges mir-34a-5p to promote colorectal cancer invasion and metastasis via hexokinase-1-mediated glycolysis[J]. Cancer Sci. 2020;111(10):3938–52.
36. Liang J, Yang Y, Bai L, et al. Drp1 upregulation promotes pancreatic cancer growth and metastasis through increased aerobic glycolysis[J]. J Gastroenterol Hepatol. 2020;35(5):885–95.
37. Gong X, Tang H, Yang K. Per1 suppresses glycolysis and cell proliferation in oral squamous cell carcinoma via the per1/rack1/pi3k signaling complex[J]. Cell Death Dis. 2021;12(3):276.
38. Baserga R. The igf-i receptor in cancer research[J]. Exp Cell Res. 1999;253(1):1–6.
39. Han L. Mir-99a inhibits proliferation and migration of cervical cancer cells by targeting igf1r[J]. J buon. 2021;26(5):1782–8.
40. Sin STK, Li Y, Liu M, et al. Trop-2 exhibits tumor suppressive functions in cervical cancer by dual inhibition of igf-1r and alk signaling[J]. Gynecol Oncol. 2019;152(1):185–93.
41. Kiely PA, Sant A, O'Connor R. Rack1 is an insulin-like growth factor 1 (igf-1) receptor-interacting protein that can regulate igf-1-mediated akt activation and protection from cell death[J]. J Biol Chem. 2002;277(25):22581–9.
42. Caromile LA, Dortche K, Rahman MM, et al Psma redirects cell survival signaling from the mapk to the pi3k-akt pathways to promote the progression of prostate cancer[J]. Sci Signal, 2017, 10(470).
43. He X, Wang J, Messing EM, et al. Regulation of receptor for activated c kinase 1 protein by the von hippel-lindau tumor suppressor in igf-i-induced renal carcinoma cell invasiveness[J]. Oncogene. 2011;30(5):535–47.
44. Wu Q, Ma J, Wei J, et al. Foxd1-as1 regulates foxd1 translation and promotes gastric cancer progression and chemoresistance by activating the pi3k/akt/mtor pathway[J]. Mol Oncol. 2021;15(1):299–316.
45. Li ZQ, Qu M, Wan HX, et al. Foxk1 promotes malignant progression of breast cancer by activating pi3k/akt/mtor signaling pathway[J]. Eur Rev Med Pharmacol Sci. 2019;23(22):9978–87.
46. Zheng Y, Wu C, Yang J, et al. Insulin-like growth factor 1-induced enolase 2 deacetylation by hdac3 promotes metastasis of pancreatic cancer[J]. Signal Transduct Target Ther. 2020;5(1):53.

47. Wang SM, Tie J, Wang WL, et al. Pou2f2-oriented network promotes human gastric cancer metastasis[J]. Gut. 2016;65(9):1427–38.
48. Bentrari F, Chantôme A, Knights A, et al. Oct-2 forms a complex with oct-1 on the inos promoter and represses transcription by interfering with recruitment of rna polii by oct-1[J]. Nucleic Acids Res. 2015;43(20):9757–65.

Tables

Table 1. RACK1 expression in cervical carcinoma according to patient's histopathologic characteristic

Characteristics	N	Negative	Weak	Moderate	Strong	χ^2	P
Cervical Cancer Tissues	104	16	24	43	16		
Cervicitis Tissues	31	24	6	0	1	39.223	<0.001
Differentiation							
Well	20	1	1	10	8		
Moderate /poor	84	13	33	23	15	10.502	0.015
L/N metastasis							
Negative	80	17	34	21	8		
Positive	24	4	9	3	8	8.350	0.039
FIGO stage							
≤IIB	90	13	23	38	16		
> IIB	14	5	5	1	3	4.218	0.239
Tumor size							
< 2.5 cm	60	14	27	12	7		
≥ 2.5 cm	44	7	16	12	9	3.219	0.359

Figures

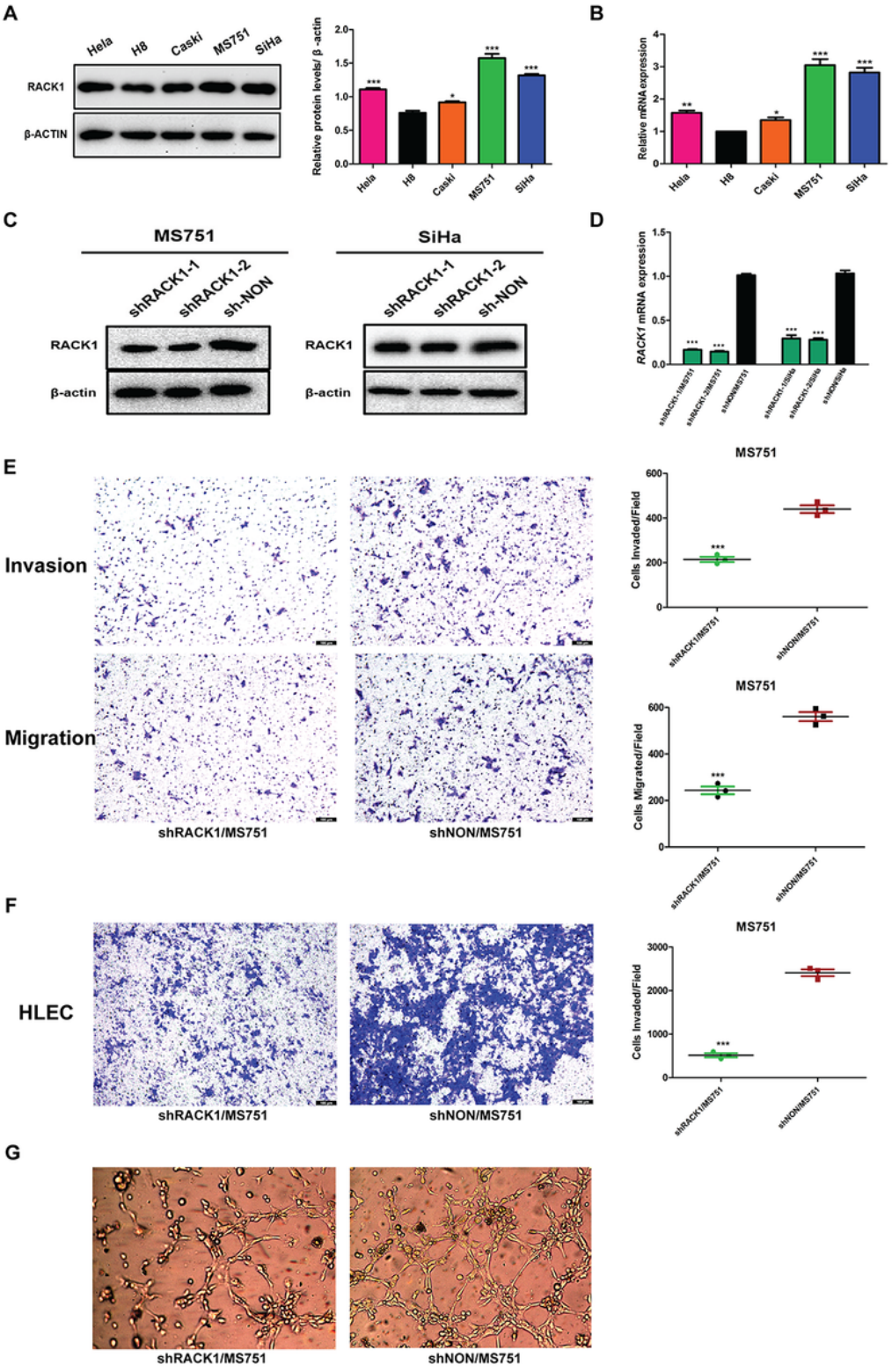

Figure 1

RACK1 is highly expressed in cervical cancer cell lines and regulates cervical cancer cell migration and invasion in vitro.

a Protein levels of RACK1 in CC cell lines (HeLa, SiHa, Caski, and MS751) and normal cell line (H8) detected by western blot analysis, with the protein bands assessed (right panel). **b** RACK1 mRNA level in

CC cell lines (HeLa, SiHa, Caski, and MS751) and normal cell line (H8) detected by qRT-PCR. **c** RACK1 expression in MS751 and SiHa cells transfected with specific shRACK1 lentiviral vectors (shRACK1-1 and shRACK1-2) was analyzed by Western blotting and **d** qRT-PCR. **e** Transwell assays were performed to investigate the effects of RACK1 on the invasion and migration of MS751 cells, with the quantified bands assessed (×100). **f** Transwell assays were performed to investigate the effects of RACK1 on the migration ability of HLECs(×100), with the quantified bands assessed(right panel). **g** Effects of RACK1 on tube formation by HLECs (×200). All data were obtained from three independent experiments. Data are presented as the mean ± SD values ($n \geq 3$). *P < 0.05, **P < 0.01, ***P < 0.001, ****P <0.0001.

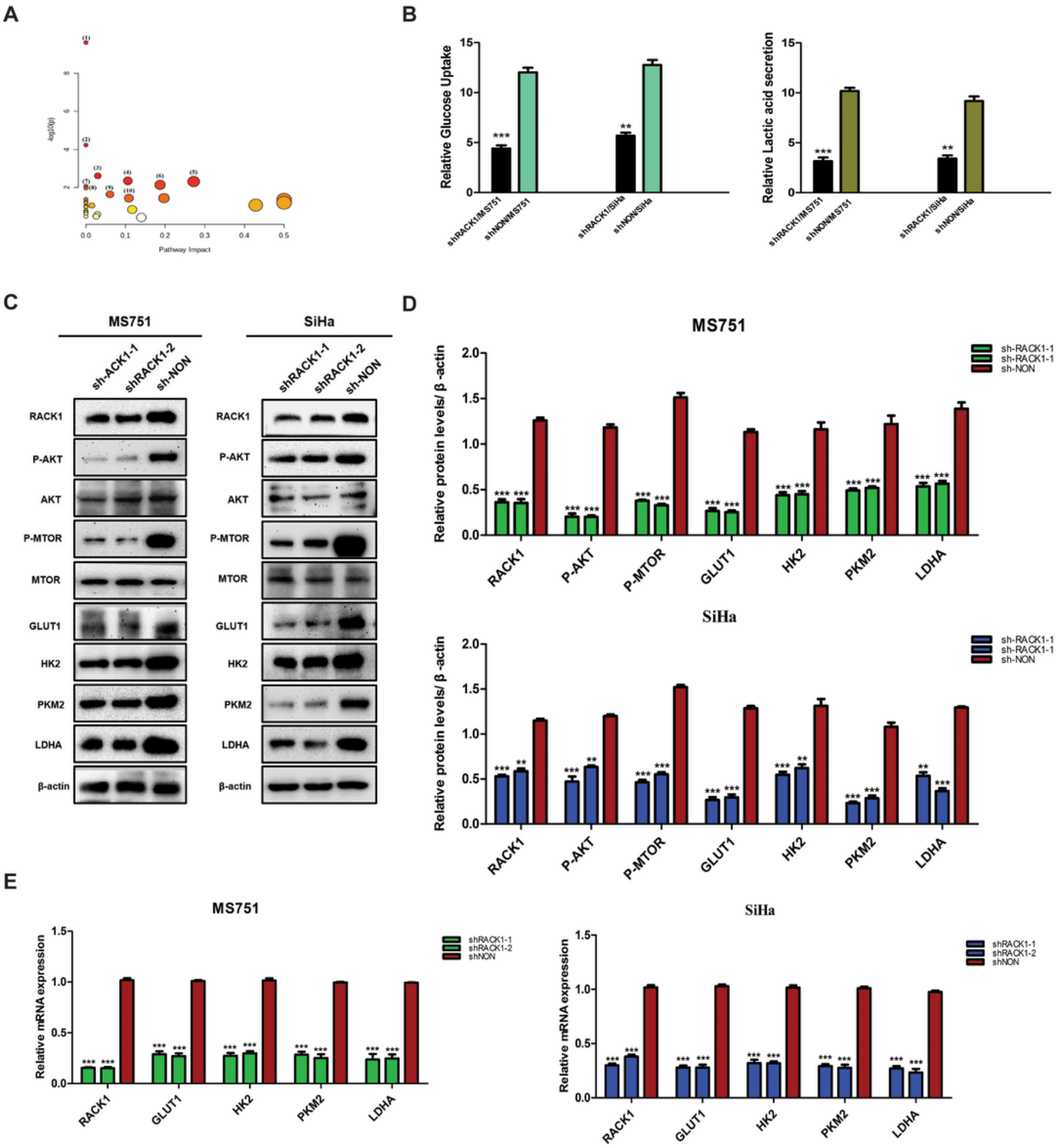

Figure 2

RACK1 enhanced the glycolysis in cervical cancer cells.

a Common differential metabolites in the metabolic pathway of the supernatant of shRACK1/MS751 and shRACK1/SiHa cells. **b** Effect of RACK1 on glucose uptake and lactate production. **c** Effect of RACK1 on the expression of the AKT/mTOR pathway, HK2, PKM2, GLUT1, and LDHA, as evaluated by western blot

analysis. **d** The bar graph summarizes the protein bands assessed. **e** Effect of RACK1 on the mRNA expression of the HK2, PKM2, GLUT1, and LDHA, as evaluated by qRT-PCR analysis. All data were obtained from three independent experiments. Data are presented as the mean ± SD values (n ≥ 3). *P < 0.05, **P < 0.01, ***P < 0.001, ****P <0.0001.

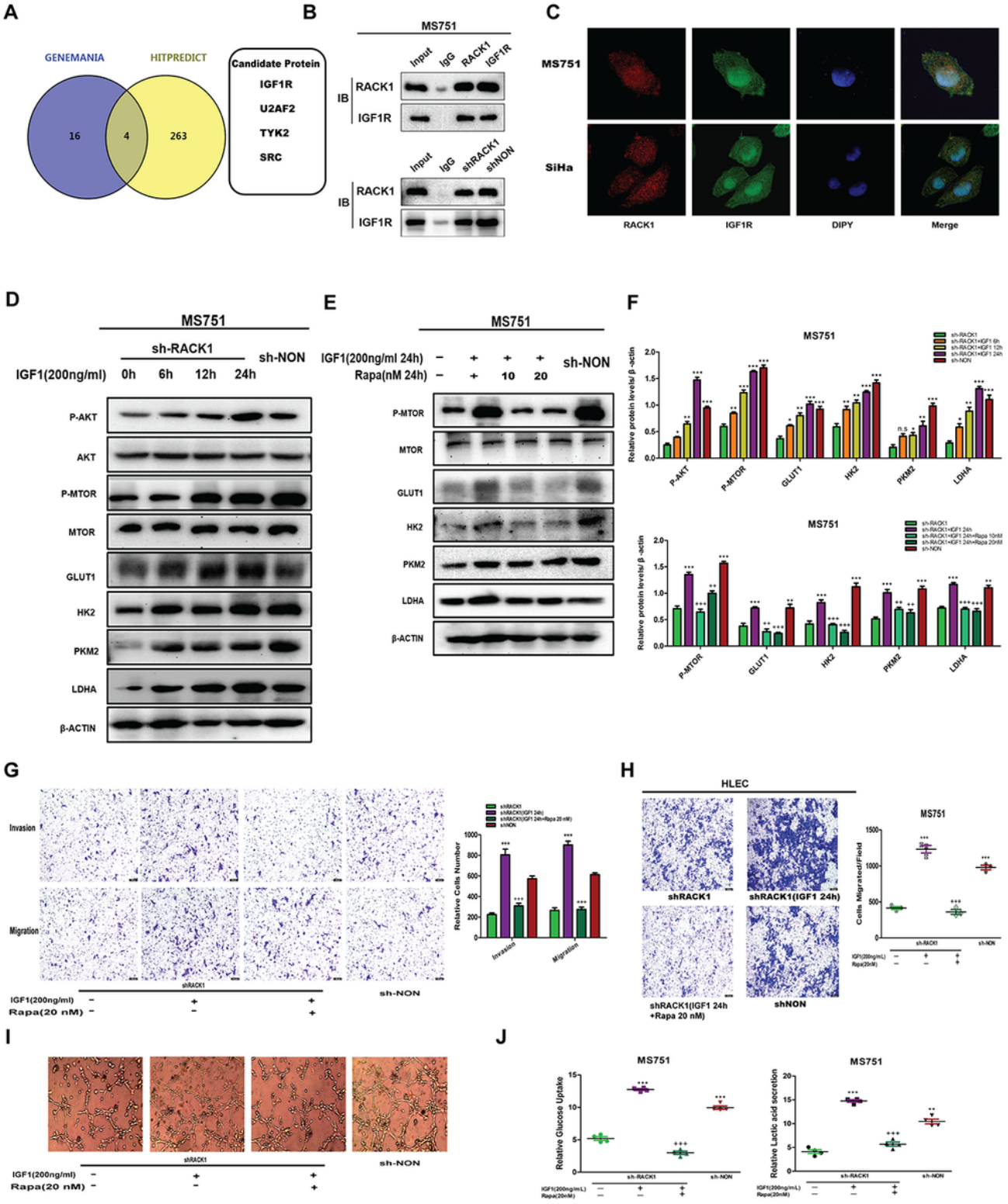

Figure 3

RACK1 interacts with IGF1R promotes the glycolysis, aggressiveness, and lymphangiogenesis by activating IGF1R/AKT/mTOR signaling in MS751 cells.

a Venn showing the factors interacting with RACK1, co-existing in the Hitpredict and Genemania databases. b Co-IP analysis of cells using anti-RACK1 and anti-IGF1R antibodies, and western blot analysis of RACK1 and IGF1R expression on MS751 cells. c Correlation between RACK1 and IGF1R expression was analyzed by immunofluorescence staining in MS751 and SiHa cells (×200). Nuclei were stained with 4’,6-diamidino-2-phenylindole (DAPI, blue). d shRACK1/MS751 cells was stimulated at different times (6 h, 12 h and 24 h) with 200 ng/mL IGF1. The AKT/mTOR pathway, HK2, PKM2, GLUT1, and LDHA expression was examined by western blot assay (n=3). e shRACK1/MS751 cells were stimulated for 24 h with 200 ng/mL IGF1 and different doses (100 nM and 200 nM) of rapamycin (RAPA). The expression of mTOR, HK2, PKM2, GLUT1, and LDHA was examined by western blotting (n=3). f The bar graph summarizes the protein bands assessed of treatment with IGF1(up panel) and IGF1 combined with RAPA(down panel). g Transwell assays were performed to investigate the effects of IGF1 and IGF1 combined with RAPA on the invasion and migration of MS751 cells, with the quantified bands assessed (right panel). h Transwell assays were performed to investigate the effects of IGF1 and IGF1 combined with RAPA on HLECs migration, with the quantified bands assessed (right panel). i Effect of IGF1 and IGF1 combined with RAPA on tube formation by HLECs (×200). j Effect of IGF1 and IGF1 combined with RAPA on glucose uptake and lactate production in MS751 cells. All data were obtained from three independent experiments. Data are presented as the mean ± SD values (n ≥ 3). *P < 0.05, **P < 0.01, ***P < 0.001, ****P <0.0001.

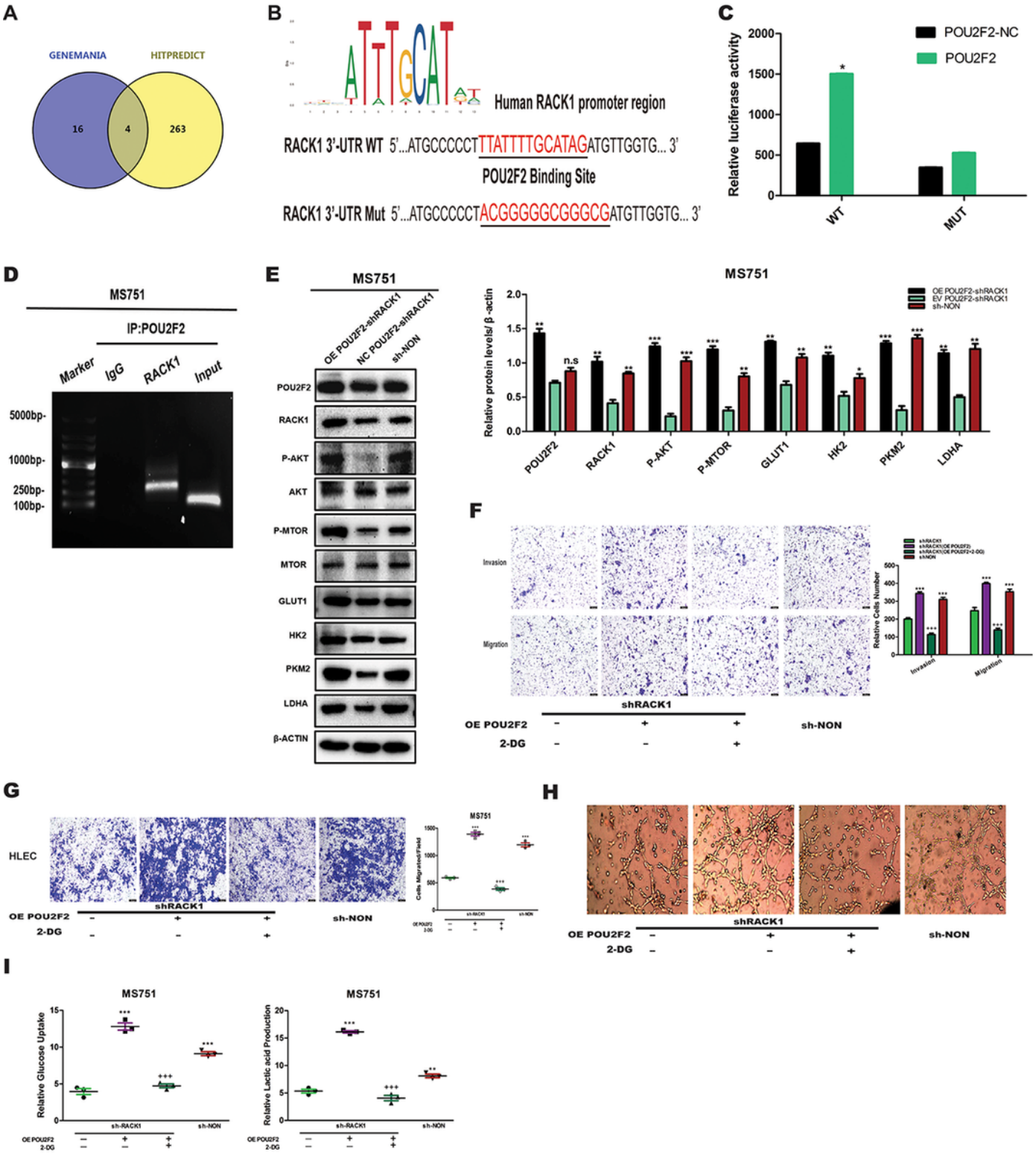

Figure 4

RACK1 is a direct target of POU2F2

a VENN showing the transcription factor binding to RACK1 co-existing in GUSC, HUMANTFDB, and PROMO database. b POU2F2 DNA binding sites are present in the human RACK1 promoter region. The top panel shows the WT and MUT forms of the putative POU2F2 target sequences in RACK1 3' -UTR. Red

font (up) refers to the putative POU2F2 targeting sequence in the RACK1 3’ -UTR. Red font (up) refers to mutations in the POU2F2 targeting sequence in RACK1 3’ -UTR. c Luciferase reporter assays of wild-type (WT) and mutated (MUT) RACK1 luciferase reporters transfected with POU2F2 in MS751 cells. d ChIP-PCR assay to detect POU2F2-binding sites in the sequence of the RACK1 promoter. e Effect of POU2F2 on the expression of AKT/mTOR pathway, HK2, PKM2, GLUT1, and LDHA in shRACK1/MS751 cells, as evaluated by western blot analysis, with the protein bands assessed (right panel). f POU2F2 OE-shRACK1/MS751 cells were stimulated for 24 h with 10 mM 2-deoxy-D-glucose (2-DG).Effect of POU2F2 and 2-DG combined with POU2F2 on the invasion and migration of shRACK1/MS751 cells, with the quantified bands assessed (right panel). g Effect of POU2F2 and 2-DG combined with POU2F2 on HLEC migration, with the quantified bands assessed (right panel). h Effect of POU2F2 on tube formation in HLECs (×200). i Effect of POU2F2 on glucose uptake and lactate production in MS751 cells. All data were obtained from three independent experiments. Data are presented as the mean ± SD values (n ≥ 3). *P < 0.05, **P < 0.01, ***P < 0.001, ****P <0.0001.

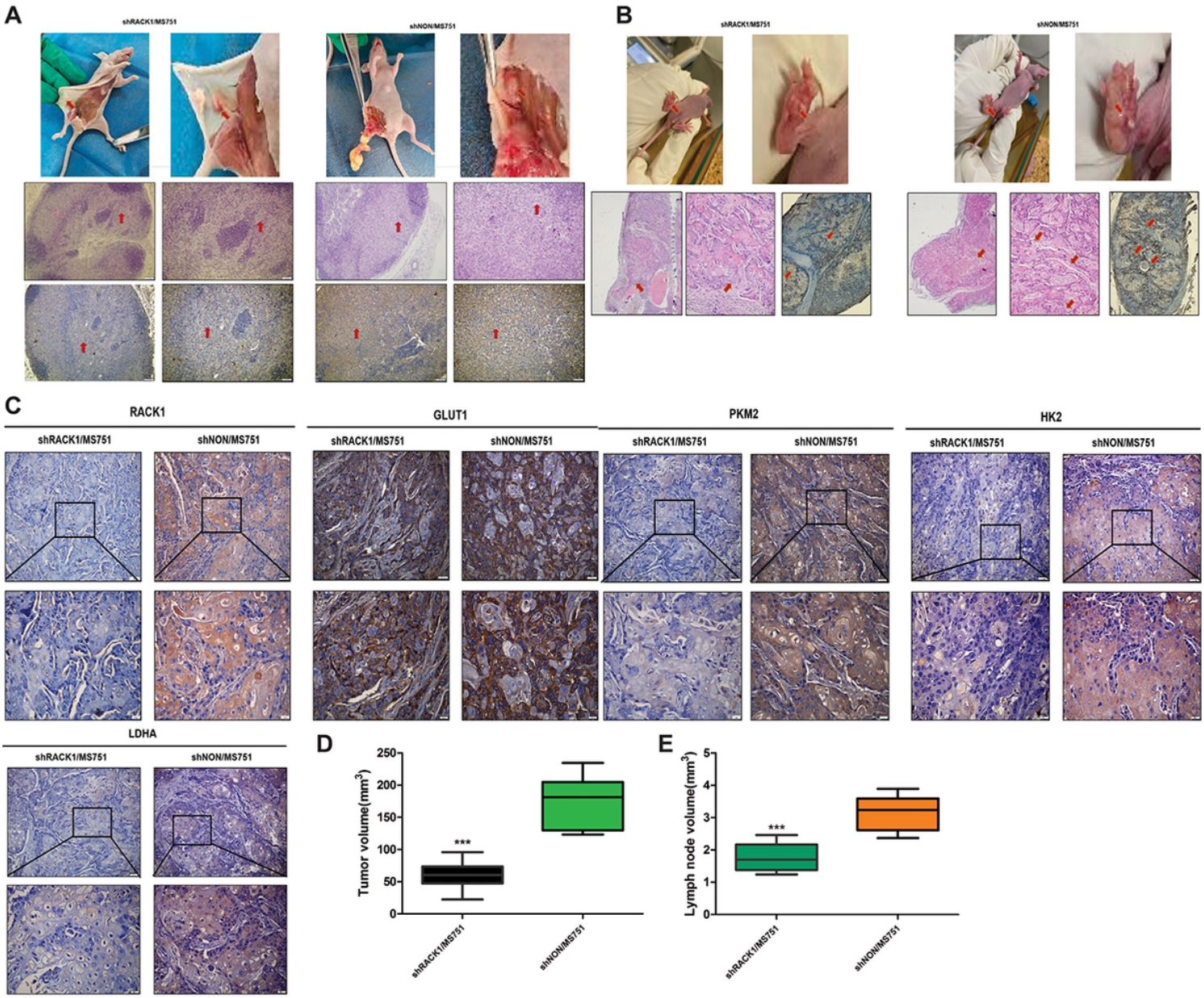

Figure 5

RACK1 enhances LNM of MS751 cells in vivo.

a Representative images of inguinal LNs in different groups of nude mice (n = 8, up panel). Representative images of inguinal LNs of HE staining in different groups of nude mice (×100 and ×200, middle panel).Representative images of anti-GFP IHC analysis for inguinal LNs in different groups of nude mice (×100 and ×200, down panel). **b** Representative images of footpads primary tumor in different groups of nude mice (n = 8, up panel). Representative images of footpads primary tumor tissues of HE staining (n =8, ×40, ×200) and percentages of PDPN-indicated lymphatic vessels density in different groups of nude mice (n =8, ×40) (down panel). **c** Representative images of LDHA, PKM2, HK2, and LDHA expressions of footpad primary tumor tissues in IHC analysis (n =8, ×200 and ×400). **d** The bar graph summarizes the tumor size assessed. **e** The bar graph summarizes the lymph node volume assessed. Data are presented as the mean ± SD values (n = 8).

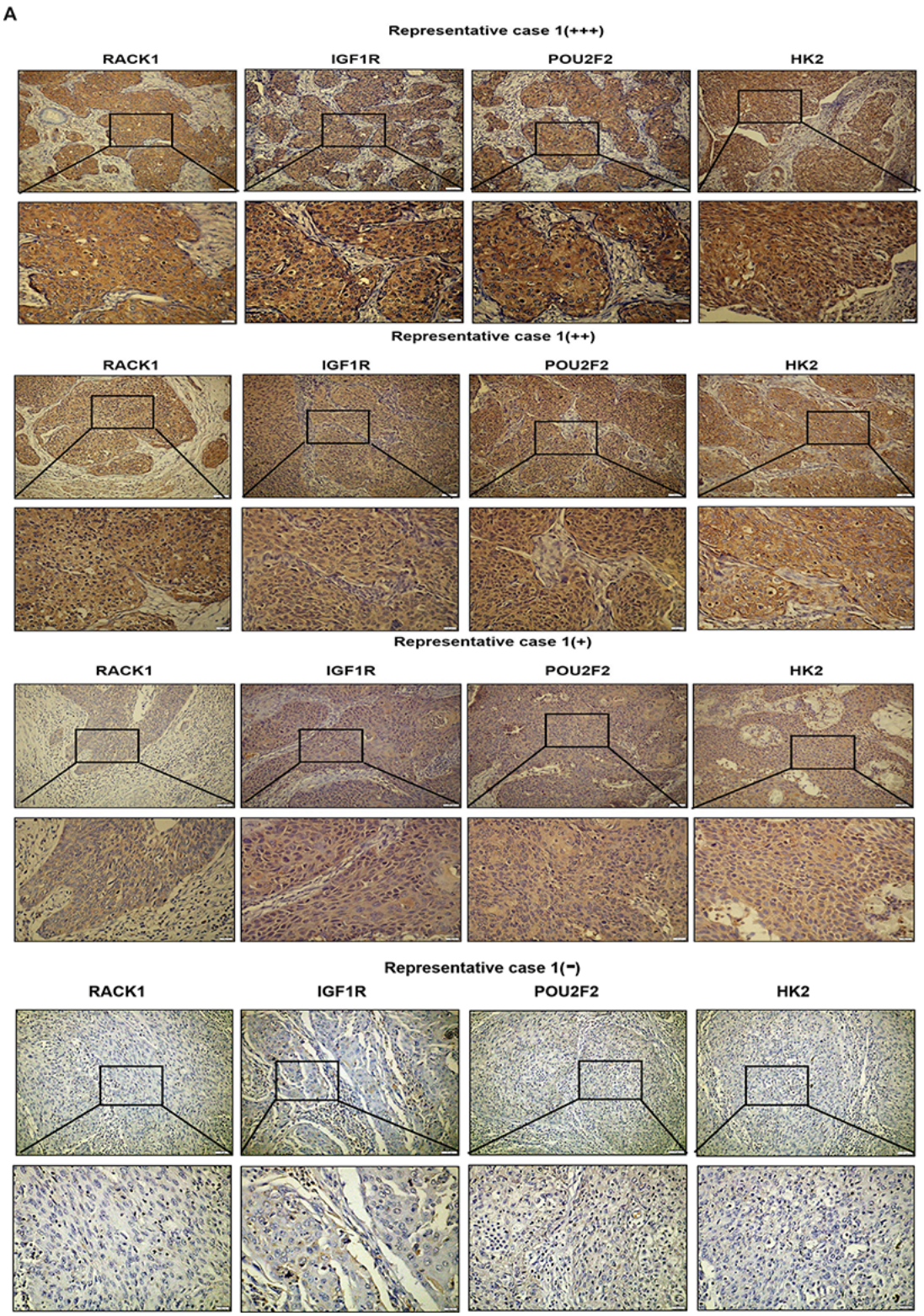

Figure 6

Associations between RACK1, IGF1R, POU2F2, and HK2 expression in patients' CC tissues.

a Representative images of IHC staining in case 1 for RACK1, IGF1R, POU2F2, and HK2 (strong RACK1 expression, ×200 and ×400). b Representative images of IHC staining in case 2 for RACK1, IGF1R, POU2F2, and HK2 (medium RACK1 expression, ×200 and ×400). c Representative images of IHC staining

in case 3 for RACK1, IGF1R, POU2F2, and HK2 (weak RACK1 expression, ×200 and ×400). d Representative images of IHC staining in case 4 for RACK1, IGF1R, POU2F2, and HK2 (negative RACK1 expression, ×200 and ×400).

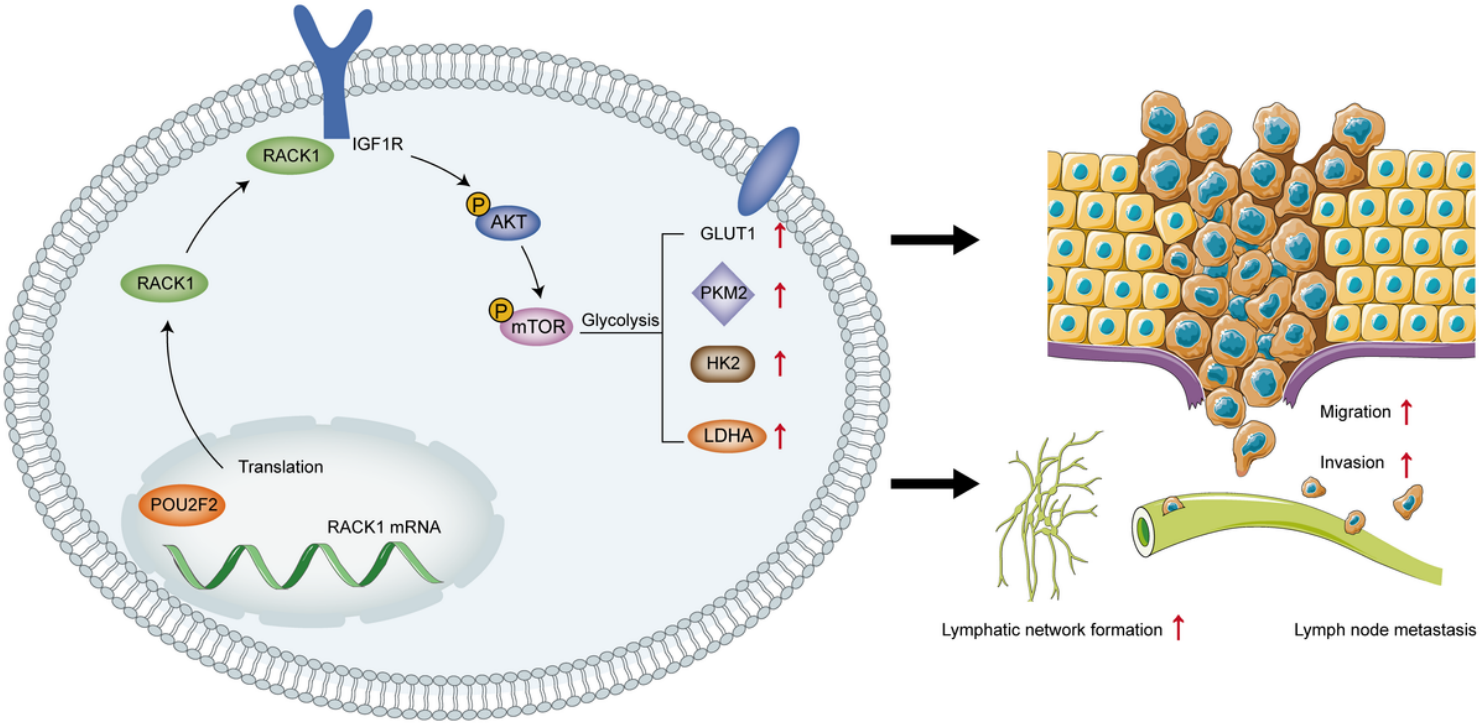

Figure 7

Schematic illustration of the mechanism by which the POU2F2/RACK1/IGF1R/AKT/mTOR promotes cell lymph node metastasis depends on glycolysis.

Supplementary Files

This is a list of supplementary files associated with this preprint. Click to download.

- FIGS1.tif
- FIGS2.tif
- FIGS3.tif
- FIGS4.tif
- FIGS5.tif
- SupplementaryTable1.docx
- SupplementaryTable2.docx
- SupplementaryTable3.docx
- SupplementaryTable4.docx

- SupplementaryTable5.docx
- SupplementaryTable6.docx
- SupplementaryTable7.docx